# GLP-1-induced AMPK activation inhibits PARP-1 and promotes LXR-mediated ABCA1 expression to protect pancreatic β-cells against cholesterol-induced toxicity through cholesterol efflux

**Rao Li**
Central South University Third Xiangya Hospital
**Xulong Sun**
Central South University Third Xiangya Hospital
**Pengzhou Li**
Central South University Third Xiangya Hospital
**Weizheng Li**
Central South University Third Xiangya Hospital
**Lei Zhao**
First Affiliated Hospital of University of South China
**Liyong Zhu** ( zly8128@126.com )
Central South University Third Xiangya Hospital
**Shaihong Zhu**
Central South University Third Xiangya Hospital

**Research**

**Keywords:** T2DM (Type 2 diabetes), GLP-1, β-cell, PARP-1, ABCA1

**Posted Date:** March 3rd, 2020

**DOI:** https://doi.org/10.21203/rs.3.rs-15784/v1



**Version of Record:** A version of this preprint was published at Frontiers in Cell and Developmental Biology on July 7th, 2021. See the published version at https://doi.org/10.3389/fcell.2021.646113.

# Abstract

**Background:** T2DM (Type 2 diabetes) is a complex, chronic disease characterized as insulin resistance and islet β-cell dysfunction. Bariatric surgeries, mainly Roux-en-Y gastric bypass (RYGB) surgery and laparoscopic sleeve gastrectomy (LSG), have become an important method for treating obesity and T2DM, and GLP-1 increase after bariatric surgery has been regarded as a central event in bariatric surgery-induced remission of T2DM.

**Methods:** The cell viability was examined using 3-[4,5-dimethylthiazol-2-yl]-2,5-diphenyl tetrazolium bromide (MTT). Cell apoptosis was determined by Flow cytometry. The cellular contents of cholesterol in INS-1 cells were measured using cholesterol assay kits. The BODIPY-cholesterol assay was performed to monitor the cholesterol efflux.

**Results:** High concentration cholesterol-induced lipotoxicity was observed in INS-1 cells, including inhibited cell viability, enhanced cell apoptosis, and inhibited cholesterol efflux from INS-1 cells; in the meantime, ABCA1 protein level was decreased by cholesterol stimulation. Cholesterol-induced toxicity and ABCA1 downregulation was attenuated by GLP-1 agonist EX-4. GLP-1 induced AMPK phosphorylation during the protection against cholesterol-induced toxicity. Under cholesterol stimulation, GLP-1-induced AMPK activation inhibited PARP-1 activity, therefore attenuating cholesterol-induced toxicity in INS-1 cells. In INS-1 cells, PARP-1 directly interacted with LXR, leading to the poly(ADP-ribosyl)ation of LXRα and downregulation of LXR-mediated ABCA1 expression. In STZ-induced T2DM model in rats, RYGB surgery or EX-4 treatment improved the glucose metabolism and lipid metabolism in rats through GLP-1 inhibition of PARP-1 activity. According to clinical data, GLP-1 was significantly increased after LSG surgery on T2DM patients, and the increase in GLP-1 was closely related to the improvement of islet function.

**Conclusions:** GLP-1 inhibits PARP-1 to protect islet β cell function against cholesterol-induced toxicity *in vitro* and *in vivo* through enhancing cholesterol efflux. GLP-1-induced AMPK and LXR-mediated ABCA1 expression are involved in GLP-1 protective effects.


# Background

T2DM (Type 2 diabetes) is a complex, chronic disease during which insulin resistance initiates and islet β-cell dysfunction occurs. Islet β-cell failure is a key link in the progression of T2DM. Genetic and environmental factors can affect pancreatic islet β-cell sensitivity and ultimately lead to further progression of the disease course [1]. Glucagon-like peptide-1 (GLP-1) has been reported to improve T2DM by stimulating pancreatic β-cell secreting insulin [2, 3], inhibiting pancreatic α-cell secreting glucagon [4], and decreasing gastrointestinal motility [5] and body weight [6]. Together with its specific receptor GLP-1 receptor (GLP-1R), GLP-1/GLP-1R signaling protects pancreatic β-cells through AMPK/mTOR, PI3K, and Bax [7].

In recent years, relevant studies have shown that cholesterol accumulation in islet progenitor cells can lead to lipid toxicity, reduce insulin secretion, and lead to apoptosis of islet progenitor cells [8, 9], subsequently accelerating the deterioration of diabetes [10]. Therefore, cholesterol metabolism disorders are an important mechanism of islet dysfunction [11] and maintaining the cholesterol homeostasis would improve pancreatic β cells function. Upon excessive accumulation, the high-density lipoprotein (HDL) remove excess cholesterol out of the cells, known as cellular cholesterol efflux. Among many transporters that could modulate cholesterol efflux, the ATP-binding cassette transporter A1 (ABCA1) has been regarded as the major one [12]. The liver X receptor (LXR) could transcriptionally and post-transcriptionally regulate ABCA1 expression; more importantly, the direct interaction of liver X receptor (LXRβ) with ABCA1 promotes the formation of HDL [13, 14]. In mice, the uptake of low-density lipoprotein (LDL) receptor (LDLr)-mediated cholesterol into pancreatic β-cells strongly affects islet cholesterol levels and β-cell function, while ABCA1-mediated cholesterol efflux could simultaneously compensate for hypercholesterolemia to balance islet cholesterol levels *in vivo* [15]. However, whether LXR-mediated ABCA1 expression also plays a role in regulating the body's blood glucose homeostasis is unclear.

PARP (Poly ADP-ribose polymerase) gene plays a critical role in inducing the damage of diabetic islet cells. In Streptozotocin (STZ)-induced diabetic mouse model, DNA damage and PARP activation in islet cells cause islet cell apoptosis, islet destruction, and increased blood glucose, while in $PARP^{-/-}$ mice, normal blood glucose and islet structure were observed, indicating that deletion of PARP can completely protect STZ-induced diabetes [16]. It is worth noting that there is an antagonism between PARP and GLP-1. For example, in human small intestinal endocrine cells NCI-H716, down-regulation of PARP activity promotes GLP-1 expression [17]; in vascular endothelial cells, GLP-1 effectively inhibits PARP-1 expression and causes loss of PARP-1/iNOS/NO pathways, thereby protecting microvascular endothelial cells [18]; AMPK downstream of GLP-1 can rapidly inhibit PARP activity and reduce its ability to regulate downstream genes [19, 20]. In addition, PARP-1 also plays an important role in LXR-regulated liposome homeostasis. For example, PARP-1 regulates cholesterol efflux in macrophages by inhibiting LXR-mediated ABCA1 expression [21]. The PARP inhibitor 3-aminobenzamide enhances ABCA1 expression in macrophages and mediates cholesterol flow to apolipoprotein AI lacking lipid [19, 20]. However, the effects of PARP-1 on LXR-mediated ABCA1 expression and cholesterol efflux from β-cells remain unknown. Therefore, we speculated that in islet cells, GLP-1 inhibits PARP-1 after activating AMPK, and down-regulation of PARP activity increases LXR transcriptional activity, so ABCA1 expression increases, promotes cholesterol outflow, and reduces cholesterol-induced cytotoxicity.

Notably, conventional therapies including antidiabetic drug therapy seemly only slow down but not stop T2DM progression and surely not heal the disease. Comparatively, a series of bariatric surgeries, mainly Roux-en-Y gastric bypass (RYGB) surgery and laparoscopic sleeve gastrectomy (LSG), have become an important method for treating obesity and T2DM in recent years, especially for cases where the curative effect of the standardized medical treatment is not satisfactory [22-24]. A study on 35 T2DM patients received bariatric surgery (23 RYGB and 12 SLG) indicated that bariatric surgery increased the insulin secretion rates and concentrations, modestly improved β-cell sensitivity and rate sensitivity, and

enhanced glucagon and GLP-1 response [25]. After RYGB, the GLP-1 concentrations in postprandial plasma were remarkably increased [26]. Since GLP-1 is an incretin hormone playing an antidiabetic role, GLP-1 increase after bariatric surgery has also been regarded as a central event in RYGB-induced remission of T2DM.

To validate the above-described speculation, we examined the effects of GLP-1 on ABCA1 expression and cholesterol-induced toxicity in islet β INS-1 cells, and the involvement of AMPK. Next, the effects of GLP-1-induced AMPK activation on PRPR-1 activity and ABCA1 expression were examined. INS-1 cells were then treated with AMPK agonist-treated and/or PARP-1 under cholesterol stimulation and the dynamic effects were monitored. The interaction between PARP-1 and LXR was verified and the effects of PARP-1 on LXR-mediated ABCA1 expression were determined. To further validate the *in vitro* findings, we established STZ-induced T2DM model in rats and performed RYGB surgery on T2DM rats or treated T2DM rats with GLP-1R agonist EX-4, and examined glucose metabolism- and lipid metabolism-related indicators. Finally, we analyzed clinical data collected from T2DM patients received LSG surgery. In summary, we attempt to provide a novel mechanism by which increased GLP-1 after bariatric surgery increases LXR-mediated ABCA1 expression through inhibiting PARP-1 activity, therefore protecting INS-1 cells from cholesterol-induced toxicity.

# Materials And Methods

### Cell line and cell treatment

INS-1 cells were obtained from the National Infrastructure of Cell Line Resource (Beijing, China) and cultured in RPMI-1640 (Invitrogen, Carlsbad, CA, USA) added with L-glutamine, FBS (10%; Invitrogen), HEPES (10 mmol/L; Sigma, St. Louis, MO, USA), sodium pyruvate (1 mmol/L; Invitrogen), and β-mercaptoethanol (50 μmol/L; Sigma-Aldrich, St. Louis, MI, USA) at 37℃ in 5% $CO_2$.

For high-fat induction, cholesterol (Santa Cruz Biotechnology; Dallas, TX, USA) was dissolved in chloroform and diluted to 2.5, 5 and 10 mM/L with culture medium for 24h; For GLP-1 treatment, cells were treated with GLP-1 agonist 5nM/L exendin-4 (Ex-4) for 24h; For AMPK activation or inhibition, cells were pre-treated with 0.5 mmol/L Acadesine (AICAR) or 10 μM/L compound c for 4 h and then co-treated with Ex-4 for 24 h, respectively.

### Cell transfection

PARP-1 knockdown was generated in target cells by the transfection of si-PARP-1 synthesized by GenePharma (Shanghai, China). PARP-1 overexpression was generated in target cells by the transfection of PARP-1-pcDNA3.1 overexpression vector by (GenePharma). The transfection into target cells was performed with the help of lipofectamine 3000 (Invitrogen). Twenty-four hours later, the transfected cells were harvested for different experiments.

### Cell viability evaluation

The cell viability was examined using 3-[4,5-dimethylthiazol-2-yl]-2,5-diphenyl tetrazolium bromide (MTT) according to the methods described before [27]. MTT is taken up by cells through the plasma membrane potential and then reduced to formazan by intracellular NAD(P)H-oxidoreductases and the formazan was dissolved by DMSO after the supernatant was discarded. OD values were measured at 490 nm and the viability was calculated taking the non-treated cell (control) viability as 100%.

### Cell apoptosis evaluation

Cell apoptosis was determined by Flow cytometry. The cells were digested by trypsin and collected. After resuspended in 100 μl binding buffer, the cells were added with 5 μl Annexin V-FITC and 5 μl Propidium Iodide (PI) at room temperature avoid of light for 15 min. Then, the cells were tested on flow cytometry.

### Immunoblotting

The total protein was extracted, resolved on 10% SDS-PAGE, and transferred onto polyvinylidene fluoride (PVDF) membranes. Non-specific bindings were blocked by an incubation with 5% nonfat dry milk in Tris buffered saline Tween (TBST) for 2 h followed by an incubation with the appropriate primary antibodies at 4°C overnight and another incubation with the appropriate secondary antibodies for 2 h at room temperature. The primary antibodies used are as follows: anti-ABCA1 (ab18180; Abcam, Cambridge, UK), anti-PARP-1 (13371-1-AP; Proteintech, Wuhan, China), anti-p-PARP-1 (MBS9206900; MyBioSource, San Diego, CA, USA), anti-LXRβ (ab28479; Abcam), anti-AMPK (10929-2-AP; Proteintech), anti-p-AMPK (ab133448; Abcam). The immunoreactive proteins were visualized and examined using an enhanced chemiluminescence reagent (ECL; BeyoECL Star Kit, Beyotime, Shanghai, China).

### Polymerase chain reaction (PCR)-based analyses

Total RNA was extracted, processed, and examined for the expression of target genes according to a method described previously [28]. The expression levels of target genes were detected by SYBR green PCR Master Mix (Qiagen, Hilden, Germany) taking GAPDH as an endogenous control. The data were processed using a $2^{-\Delta\Delta CT}$ method.

### Measurements of cellular cholesterol

The cellular contents of cholesterol in INS-1 cells were measured using cholesterol assay kits (ab133116; Abcam) according to the manufacturers' protocol.

### Determination of adipogenic induction

After treatment and/or transfection, to identify the lip droplets in cells, INS-1 cells were fixed in paraformaldehyde (4%), stained with oil red O (0.5%; Santa Cruz, Dallas, TX, USA), and observed for images under an inverted light microscope. For Bodipy staining, fixed cells were stained with Bodipy solution (1 μg/ml) and observed for images under fluorescence microscope.

## Cholesterol efflux from INS-1 cells

The BODIPY-cholesterol assay was performed to monitor the cholesterol efflux from INS-1 cells following the methods described previously [29]. Cells were planted in black 96-well plates at a density of $2\times10^4$ cells/well and cultured for 24 h. Then, cells were treated with cholesterol (without cholesterol as the control group) for 1 h and replaced with serum-free medium for 24 h followed by another incubation with EX-4 for 1 h. Next, cells were cultured in serum-free medium containing labeling media, which is consisted of BODIPY cholesterol (0.025 mM) (TopFluor® Cholesterol, product No. 810255; Avanti Polar Lipids, Ablaster, AL, USA), MCD (10 mM), HEPES (Sigma), and egg phosphatidylcholine (0.1 mM) (Avanti Polar Lipids) [29] for 1 h. Cells were washed with RPMI-1640 and incubated with serum-free medium for 18 h. Then, cells were observed by After that, cells were dissolved with 1% cholic acid (Sigma) in 1N NaOH for 4 h under agitation while the supernatant was collected and then centrifuged at 10,000 ×g for 5 min. The fluorescence intensity representing the cholesterol was examined using a microplate reader at an excitation wavelength of 482 nm and an emission wavelength of 515 nm. The percentage of the cholesterol efflux was calculated as cholesterol efflux intensity/(intracellular cholesterol + cholesterol efflux) ×100%.

## Co-Immunoprecipitation (Co-IP) assay

The sequence encoding LXR and PARP-1 were cloned into the pcDNA3.1/Flag or pcDNA3.1/His vector, named Flag-LXR and His-PARP-1, respectively. Then, these vectors were co-transfected into INS-1 cells. Empty vectors were co-transfected into target cells as controls. Thirty-six hours after transfection, the cells were harvested and the proteins were extracted. Flag monoclonal antibodies were used for IP testing followed by Immunoblotting using anti-Flag (ab49763; Abcam) and anti-His (ab5000; Abcam) antibodies. In order to exclude the effect of DNase and RNase, we treated the cell lysates with 5mg/ml Dnase and Rnase, respectively.

## Poly(ADP-ribosyl)ation Assay

To examine poly(ADP-ribosyl)ation (also known as PARylation, is a special case of ADP-ribosylation), recombinant full-length human GLP-1 (100 ng; Abcam) was incubated with recombinant human PARP-1 (40 ng; 31238; Active Motif, Carlsbad, CA, USA) with the pre-treatment of AMPK activator AICAR or AMPK inhibitor Compound C under cholesterol treatment, or recombinant full-length human LXRα (100 ng; Protein One, Rockville, MD, USA) was incubated with recombinant human PARP-1 (40 ng; 31238; Active Motif) in the reaction buffer described previously [21] for 30 min. The reaction was terminated as described and the poly(ADP-ribosyl)ation was visualized by immunoblotting with anti-PAR1 antibody [21].

## Diabetes mellitus rat models and Roux-en-Y gastric bypass (RYGB) surgery

Six-week-old male SD rats (n = 50) were obtained from SLAC Laboratory Animal Co., Ltd. (Shanghai, China) and randomly assigned into five groups: non-treatment control group, streptozotocin (STZ)-induced T2DM group, STZ-induced T2DM plus sham surgery group, STZ-induced T2DM plus RYGB

surgery group, and STZ-induced T2DM plus EX-4 treatment group. T2DM was induced by the intraperitoneal (i.p.) injection of 60 mg/kg STZ (Sigma) after overnight fasting. Rats in the non-treatment control group were injected with an equal volume of PBS in citrate buffer solution (pH 4.5). Before surgery, all rats were fasted overnight and then intraperitoneally anesthetized with chloral hydrate (10%, 350 mg/kg; Sigma). The RYGB surgery was performed on rats following the methods reported before [30].

### Blood sample collection and examination

For animal experiments, blood was collected from rat tail veins prior to and 1, 2, 4, and 8 weeks after surgery. For blood sample collection, rats in different groups were euthanized through intraperitoneal injection of sodium pentobarbital (150 mg/kg; Sigma). GLP-1 and insulin levels in clinc samples and rat blood were determined by ELISA using GLP-1 (cat. no. RA20061; Bio-Swamp Life Science, Wuhan, China) and insulin (cat. no. RA20092; Bio-Swamp Life Science) kits following the manufacturer's instructions. The levels of total cholesterol (TC), triglyceride (TG), low-density lipoprotein cholesterol (LDL-C), and high-density lipoprotein cholesterol (HDL-C) were determined using an automatic biochemical analyzer (BS-450; Mindray, Nanshan, Shenzhen, China).

### Clinical data collection

Ten cases of T2DM patients received LSG treatment in the Third Xiangya Hospital of Central South Uniersity were enrolled. The data collection was performed with the approval of the Ethics Committee of the Third Xiangya Hospital of Central South Uniersity. All patients signed informed consent forms. Oral glucose tolerance test (OGTT) was measured before LSG surgery and 3 months after surgery. PG, INS, C peptide, and GLP-1 were examined before oral glucose and 30 minutes, 60 minutes, and 120 minutes after oral glucose. Disposition Index (DI) = (Ins30−Ins0)/(Glu30−Glu0)*1/HOMA-IR, Insulin Sensitivity Index (IAI) = 1/(FINSXFPG), Insulinogenic index = (Ins30−Ins0)/(Glu30−Glu0), HOMA-β = 20*FINS/(FPG-3.5). The correlation between the area under the curve (AUC) of GLP-1 and the area under the curve of blood glucose and C-peptide was analyzed,

### Hematoxylin and eosin (H&E) and immunohistochemical (IHC) staining

Formalin fixed and paraffin-embedded rats' pancreatic tissue sections were deparaffinized in xylene and rehydrated using graded ethanol into PBS. Endogenous peroxidase is blocked with 0.3% hydrogen peroxide in methanol. For histopathological evaluations, the sections were stained with H&E. For the protein content and distribution, the sections were applied for IHC staining. Sections were incubated with 5% normal rat serum followed by another incubation firstly with primary antibodies against ABCA1 and PARP-1 at 4°C overnight, secondly with a biotinylated secondary antibody, and thirdly with an avidin-biotinylated peroxidase complex (Santa Cruz Biotechnology).

### Data processing and statistical analysis

The data were analyzed with GraphPad software. The measurement data were expressed as mean ± standard deviation (SD). Among-group and intra-group data comparisons were performed with the ANOVA and Student's *t*-tests. $P<0.05$ indicated statistically significant difference.

# Results

### GLP-1 upregulates ABCA1 expression to inhibit cholesterol accumulation-induced toxicity in INS-1 cells

It has been reported that GLP-1 agonist EX-4 could induce ABCA1 protein expression thought increasing ABCA1 promoter activity in INS-1 cells, therefore protecting INS-1 cells from cholesterol accumulation-induced β-cells dysfunction [31]. In the present study, we first verified the effects of GLP-1 on ABCA1 expression and cholesterol accumulation-induced toxicity in INS-1 cells.

INS-1 cells were cultured in different concentrations of cholesterol (0, 1, 2.5, and 5 mM) for 24 h. As shown in Fig.1A-C, cholesterol stimulation inhibited the cell viability, promoted the cell apoptosis, and decreased the protein levels of ABCA1 in a concentration-dependent manner, indicating the occurrence of cholesterol-induced toxicity in INS-1 cells.

Next, INS-1 cells were cultured in medium containing 5 mM cholesterol in the presence or absence of 5 nM Exendin-4 (EX-4; GLP-1 agonist) for 24 h. Cholesterol-caused suppression on the cell viability (Fig.1D) and the protein levels of ABCA1 (Fig.1F), and cholesterol-induced cell apoptosis (Fig.1E) were all reversed by EX-4 co-treatment. Moreover, cholesterol stimulation significantly increased the intracellular cholesterol concentration while EX-4 co-treatment reduced cholesterol-induced increase in intracellular cholesterol content (Fig.1G); Oil Red O and BODPIY staining showed that in cholesterol-stimulated INS-1 cells, lipid droplet accumulation was dramatically increased compared to that in the control group while decreased after EX-4 co-treatment compared to that in the single cholesterol group (Fig.1H). In the meantime, the BODIPY-cholesterol efflux assay indicated that EX-4 co-treatment dramatically increased cholesterol efflux from INS-1 cells compared to single cholesterol stimulation group or the control group (Fig.1I). All the results indicated that GLP-1 agonist EX-4 improves cholesterol accumulation-induced toxicity and maintains cholesterol homeostasis in INS-1 cells by increasing the cholesterol efflux from INS-1 cells.

### AMPK signaling is involved in GLP-1 regulation of ABCA1 expression and cholesterol-induced toxicity

AMPK-dependent PARP1 inhibition participate in the endothelial protection under the conditions of anti-hypertensive and anti-diabetic drugs [20]. Next, we investigated whether AMPK signaling is involved in GLP-1 protection of INS-1 cells against cholesterol-induced toxicity. As shown in Fig.2A, cholesterol stimulation significantly decreased, while EX-4 treatment increased the phosphorylation of AMPK in INS-1 cells, suggesting the involvement of AMPK signaling. Next, INS-1 cells under cholesterol stimulation were treated with EX-4 in the presence of AMPK activator AICAR or AMPK inhibitor Compound C and examined for related indexes. Under cholesterol stimulation, EX-4-rescued ABCA1 protein levels and cell viability were further promoted by AMPK activator AICAR but inhibited by AMPK inhibitor Compound C (Fig.2B-C).

Consistently, under cholesterol stimulation, EX-4-suppressed cell apoptosis was further suppressed by AMPK activator AICAR but promoted by AMPK inhibitor Compound C (Fig.2D). As for the lipid droplet accumulation, cholesterol stimulation-induced lipid droplet accumulation was attenuated by EX-4 and further attenuated by AMPK activator AICAR but enhanced by AMPK inhibitor Compound C (Fig.2E). Regarding the intracellular cholesterol homeostasis, EX-4-induced cholesterol efflux from INS-1 cells was further enhanced by AMPK activator AICAR but inhibited by AMPK inhibitor Compound C (Fig.2F). These data indicate that AMPK activation enhances GLP-1 protection of INS-1 cells against cholesterol-induced toxicity.

### GLP-1 regulates ABCA1 expression through AMPK-dependent inhibition on PARP1 activity

By using NAD+ as a substrate, a process called PARylation occurs, during which PAR is synthesized by PARP1, cellular NAD+ and ATP are depleted, and transcription factors such as NF-κB are activated [32-35]; thus, the protein level of PAR could be considered as a mark of PARP1 activity. Next, we examined the specific effects of AMPK phosphorylation on PARP1 activity and ABCA1 expression. We cultured cholesterol-stimulated INS-1 cells with GLP-1 with the pre-treatment of AMPK activator AICAR or AMPK inhibitor Compound C to examine whether AMPK activation could repress PARP1 activity and consequent PARylation. With GLP-1 treatment, cholesterol-induced increase in the protein level of PAR was decreased in INS-1 cells compared to that in single cholesterol stimulation group (Fig.3A). Pre-treatment with AICAR significantly enhanced, while pre-treatment with Compound C attenuated the suppressive effects of GLP-1 on PAR protein level (Fig.3A). These data suggest that AMPK activation enhances GLP-1-caused suppression on PARP-1 activity upon cholesterol stimulation.

To further confirm the involvement of AMPK-dependent inhibition on PARP-1 activity in GLP-1 regulation of ABCA1 expression, we generated PARP-1 knockdown in INS-1 cells by the transfection of si-PARP-1. The transfection efficiency was confirmed by Immunoblotting (Fig.3B). Cholesterol-stimulated INS-1 cells were transfected with si-PARP-1 or treated with PARP-1 inhibitor 3-AB and the ABCA1 protein level was examined; as shown in Fig.3C, the protein levels of ABCA1 were significantly increased by PARP-1 knockdown or PARP-1 inhibitor 3-AB, compared to those in the control or si-NC (negative control) group. Next, cholesterol-stimulated INS-1 cell were treated with AMPK activator AICAR or PARP-1 overexpression alone or co-treated with AICAR and PARP-1 and examined for the protein levels of p-PARP-1 and ABCA1. As shown in Fig.3D, AICAR treatment significantly inhibited the phosphorylation of PARP-1 while increased ABCA1 protein level; on the contrary, PARP-1 treatment promoted PARP-1 phosphorylation while decreased ABCA1 protein level upon cholesterol stimulation. More importantly the effects of AICAR on PARP-1 phosphorylation and ABCA1 protein level were significantly reversed by PARP-1 treatment. These data indicate that GLP-1 regulates ABCA1 protein levels through AMPK-dependent inhibition on PARP-1 phosphorylation and PAPR-1 activity.

### AMPK inhibits PARP1 activity to attenuate cholesterol-induced toxicity

We already revealed that GLP-1 increases the phosphorylation of AMPK in INS-1 to regulate ABCA1 protein level and to protect against cholesterol-induced toxicity; next, we further investigated whether

AMPK activation could attenuate cholesterol-induced toxicity through inhibiting PARP-1 activity. Cholesterol-stimulated INS-1 cells were treated with AICAR or PARP-1 alone or co-treated with AICAR and PARP-1 and examined for related indexes. AICAR significantly promoted the cell viability and inhibited the cell apoptosis in INS-1 cells, while PARP-1 exerted opposite effects; the effects of AICAR on INS-1 cells were significantly reversed by PARP-1 (Fig.4A-B). Consistently, AICAR significantly reduced, while PARP-1 promoted the intracellular lipid deposition; the effects of AICAR on the intracellular lipid deposition were reversed by PARP-1 (Fig.4C). Regarding cholesterol homeostasis, AICAR significantly increased, while PARP-1 inhibited the cholesterol efflux from INS-1 cells (Fig.4D); similarly, the effects of AICAR on cholesterol efflux from INS-1 cells were reversed by PARP-1 (Fig.4D). These data indicate that AMPK activation could attenuate cholesterol-induced toxicity; these beneficial effects of AMPK activation are inhibited by PARP-1 activation.

### PAPR-1 inhibits LXR-induced ABCA1 transcription in INS-1 cells

PARP-1 has been reported to represses LXR-mediated ABCA1 expression and cholesterol efflux in macrophages [21]; here, we investigated whether PARP-1 could also inhibit LXR-induced ABCA1 expression in INS-1 cells. In Co-IP assays, Flag-LXR and His-PARP-1 vectors were constructed and co-transfected into INS-1 cells. Results from Immunoblotting showed that PARP-1 protein could interact with LXR protein in INS-1 cells. LXRα poly(ADP-ribosyl)ation could also be detected in INS-1, and the poly(ADP-ribosyl)ation of LXRα was reduced upon inhibition of PARP-1 by 3-AB (Fig.5B). Moreover, INS-1 cells were transfected with si-PARP-1 in the presence or absence of LXR receptor agonist T0901317 and examined for the expression and protein levels of ABCA1. LXR receptor agonist T0901317 treatment dramatically promoted the expression and protein levels of ABCA1, which could be further promoted by PARP-1 knockdown; but even without LXR receptor agonist T0901317 treatment, PARP-1 knockdown alone also caused an increase in ABCA1 expression and protein level (Fig.5C). These data indicate that PAPR-1 induces LXRα poly(ADP-ribosyl)ation, therefore inhibiting LXR-induced ABCA1 expression in INS-1 cells.

### GLP-1 inhibits PARP-1 to improve islet function in T2DM rats

To further confirm these in vitro findings, we established T2DM model in Sprague-Dawley (SD) rats and performed functional analyses. SD rats were randomly assigned into five groups: non-treatment control group, streptozotocin (STZ)-induced T2DM group, STZ-induced T2DM plus sham surgery group, STZ-induced T2DM plus RYGB surgery group, and STZ-induced T2DM plus EX-4 treatment group. At pre-operation, 1, 2, 4, and 8 weeks after the last EX-4 treatment, related indexes were monitored. One week after surgery, significant weight loss was observed T2DM+RYGB group; from week 2-4, rats in all the T2DM groups had lower body weight than those in the normal group, among which the body weight of rats in T2DM+RYGB group increased slowly post-operation, slightly higher than that in T2DM and T2DM+sham, while the body weight of rats in T2DM+ EX-4 group kept stable and increased slowly (Fig.6A). FBG levels in T2DM+RYGB and T2DM+ EX-4 groups decreased significantly after surgery, while those in T2DM and T2DM+sham groups increased steadily (Fig.6B). The AUC of T2DM+RYGB and T2DM+ EX-4 group significantly decreased after surgery, while the AUC of T2DM and T2DM+sham group

was slightly decreased (Fig.6C). The TC (Fig.6D) and TG (Fig.6E) contents in T2DM+RYGB and T2DM+ EX-4 groups decreased significantly after surgery, while those in T2DM and T2DM+sham groups increased steadily. The HDL-C significantly increased in T2DM+RYGB and T2DM+ EX-4 groups after surgery while kept steady in T2DM and T2DM+sham groups (Fig.6F). The LDL-C decreased in T2DM+RYGB and T2DM+ EX-4 groups after surgery while increased steadily in T2DM and T2DM+sham groups (Fig.6G). Regarding the serum GLP-1 and insulin levels, GLP-1 levels significantly increased in T2DM+RYGB and T2DM+ EX-4 groups while only moderately changed in T2DM and T2DM+sham groups (Fig.6H); insulin content was first decreased and then increased stably in T2DM+RYGB group, continuously increased in T2DM+ EX-4 group, and decreased in T2DM and T2DM+sham groups (Fig.6I). These data all indicate that T2DM rats showed significant improvement in glucose metabolism and lipid metabolism after LSG surgery or EX-4 treatment.

At the end of the EX-4 treatment, the protein levels of p-AMPK, AMPK, PARP-1, LXRβ, and ABCA1 were examined in rats' pancreatic tissues. PARP-1 protein level was significantly increased, and p-AMPK/AMPK, LXRβ, and ABCA1 were decreased in T2DM and T2DM+sham groups; on the contrary, PARP-1 protein level was significantly decreased, and p-AMPK/AMPK, LXRβ, and ABCA1 were increased in T2DM+RYGB and T2DM+ EX-4 groups (Fig.6J). These are consistent with the in vitro results that GLP-1 induces AMPK phosphorylation, inhibits PARP-1, therefore increasing LXRβ-mediated ABCA1 expression.

To confirm the pancreatic islet morphology, we observed the pancreatic islet by H&E staining under microscope. As shown in Fig.6K, the boundary is obvious between islet and acinus in control, T2DM+RYGB, and T2DM+ EX-4 groups (Fig.6K). (K) The histopathology of rats' pancreatic tissues was examined by H&E staining. IHC staining also showed that the protein contents of ABCA1 and GLP-1 were decreased in T2DM and T2DM+sham groups while increased in T2DM+RYGB and T2DM+ EX-4 groups (Fig.6L).

### GLP-1 expression is correlated with islet function after LSG treatment on T2DM patients

To further investigate the *in vitro* findings, we analyzed clinical data from ten cases of T2DM patients received LSG treatment. OGTT was performed and related clinical indicators were examined and recorded. Three months after the LSG, the GLP-1, insulin, C-peptide, glucose, BMI, HbA1c were significantly improved in T2DM patients compared with before surgery (Table 1). In addition, the index DI, Insulinogenic index, and HOMA-β, which reflect islet function, were also significantly improved (Table 1). Furthermore, the correlations between the AUC (three months after and before LSG) of GLP-1 and that of blood glucose and c-peptide were analyzed. As shown in Fig.7A-B, $AUC_{0\text{-}120}$GLP-1 was found to be closely negatively related to $AUC_{0\text{-}120}$Glucose (r=-0.72, $P$=0.02) and $AUC_{0\text{-}120}$C-peptide (r=-0.73, $P$=0.02), respectively. These data indicate that LSG can significantly improve the blood glucose and islet function of T2DM patients, and the increase of GLP-1 after surgery is closely related to the improvement of blood glucose and islet function.

# Discussion

In the present study, high concentration cholesterol-induced lipotoxicity was observed in INS-1 cells, including inhibited cell viability, enhanced cell apoptosis, and inhibited cholesterol efflux from INS-1 cells; in the meantime, ABCA1 protein level was decreased by cholesterol stimulation. Cholesterol-induced toxicity and ABCA1 downregulation was attenuated by GLP-1 agonist EX-4. GLP-1 induced AMPK phosphorylation during the protection against cholesterol-induced toxicity. Under cholesterol stimulation, GLP-1-induced AMPK activation inhibited PARP-1 activity, therefore attenuating cholesterol-induced toxicity in INS-1 cells. In INS-1 cells, PARP-1 directly interacted with LXR, leading to the poly(ADP-ribosyl)ation of LXRα and downregulation of LXR-mediated ABCA1 expression. In STZ-induced T2DM model in rats, RYGB surgery or EX-4 treatment improved the glucose metabolism and lipid metabolism in rats through GLP-1 inhibition of PARP-1 activity. According to clinical data, GLP-1 was significantly increased after LSG surgery on T2DM patients, and the increase in GLP-1 was closely related to the improvement of islet function.

As is well-known, GLP-1 can stimulate islet β cells to secrete insulin and inhibit glucagon secretion [2-4]. In addition, GLP-1 can reduce the islet β cell apoptosis rate and stimulate β cell proliferation and regeneration [36, 37]. Lipidtoxicity is the main feature of T2DM, but the protective effect of GLP-1 regulation of cholesterol efflux from pancreatic β-cells against lipotoxicity has not been reported. In this study, we found that high fat (high concentration of cholesterol) can inhibit pancreatic β-cell cholesterol efflux, and down-regulate the expression of ABCA1 in islet INS-1 cells, while GLP-1 treatment upregulates the expression of ABCA1, therefore repairing the cholesterol efflux from islet β-cells that are damaged by lipotoxicity, reducing the cellular cholesterol content, improving cellular lipid deposition, and restoring islet β-cell function. This is similar to the results of previous studies [38, 39]. ABCA1 is a membrane protein that regulates the cellular cholesterol efflux and the outflow of lipoprotein receptors for phospholipids. Non-hepatocytes, such as pancreatic β-cells, cannot metabolize cholesterol [40]. Thus, cholesterol efflux from pancreatic islet β cells is mainly through ABCA1, which expels cholesterol out of the cells through the cell membrane to combine with cholesterol acceptor Apolipoprotein A-I (ApoA-I) [41]. ABCA1 knockout mice had impaired glucose tolerance but normal insulin sensitivity, suggesting that these mice had islet β-cell dysfunction; in the meantime, ABCA1 knockout mice had low total plasma cholesterol levels [40]. These findings all indicate that GLP-1-induced ABCA1 upregulation contributes to the cholesterol homeostasis in pancreatic β-cells and protects pancreatic β-cells from cholesterol-induced toxicity.

Cholesterol efflux has long been regarded as a critical mechanism of maintaining intracellular cholesterol homeostasis, which could be primarily regulated by the LXR transcription factors and their targeted genes, the ATP-binding cassette (ABC) cholesterol transporters ABCA1 and ABCG1 [42]. In hepatocytes, GLP-1 inhibits intracellular lipid production through the cAMP/AMPK signaling pathway, and this pathway can directly act on LXR [43]. In pancreatic β cells, GLP-1 binds GLP-1R to promote the conversion of ATP into cytoplasmic cAMP, further activating the intracellular PKA/AMPK signaling pathway and promoting glucose-stimulated insulin secretion (GSIS) [44]. The above-mentioned indirect evidence suggests that after GLP-1 binds to GLP-1R on the surface of islet β cells, it is likely to activate

the AMPK signaling pathway to act on the nucleus LXRβ, promote the activation of cell membrane ABCA1, and thus participate in the process of cholesterol efflux from islet β cells. In the present study, cholesterol-induced suppression on AMPK phosphorylation and ABCA1 protein expression could indeed be attenuated by GLP-1 agonist EX-4 and further abolished by AMPK activator AICAR while enhanced by AMPK inhibitor Compound C. Consistently, AMPK activator AICAR attenuated, while AMPK inhibitor Compound C aggravated cholesterol-induced toxicity. These data indicate that GLP-1 protects islet β cells against cholesterol-induced toxicity through activating AMPK, and LXR might be involved.

Initiated by stimuli such as oxidative stress, PARP1 activation exerts essential functions in DNA repair and maintenance of genome stability. PARP1 overexpression may in turn aggravates the oxidative stress and stimulates pro-inflammatory and necrotic responses [45]. As we have mentioned, PARP1 synthesizes PAR for "PARylation" of both itself and other proteins (nuclear and cytoplasmic) by making use of NAD+ and ATP, leading to the activation of transcription factors such as NF-κB and AP-1 [32-35]. Interestingly, PARP-1 also participates in lipid homeostasis [46]. In the present study, we first demonstrated that in islet β cells, GPL-1-induced AMPK activation suppressed PARP-1 activity to increase ABCA1 protein expression, while PARP-1 overactivation reversed the promotive effects of GPL-1-induced AMPK activation on ABCA1 protein expression. Consistently, AMPK activator AICAR attenuated, while PARP-1 overactivation aggravated cholesterol-induced toxicity in INS-1 cells, indicating that in islet β cells, PARP-1 also regulates cholesterol efflux through AMPK activation and ABCA1 protein, therefore affecting the GLP-1 protection against cholesterol-induced toxicity.

Previous study has revealed that PARP-1 could inhibit LXR-induced ABCA1 expression and cholesterol efflux from macrophages [21]. LXR (LXRα/β) is a ligand-activated transcription factor of the nuclear hormone receptor superfamily that stimulates transcription of genes involved in reverse cholesterol transport (RCT), including ABCA1 and apoE, in macrophages and intestines. PARP-1 has been reported to regulates LXR-mediated lipid homeostasis. For example, PARP-1 regulates cholesterol efflux in macrophages by inhibiting LXR-mediated ABCA1 expression [21]. In the present study, we first demonstrated the interaction between PARP-1 and LXR in islet β cells. PARP-1-induced LXRα poly(ADP-ribosyl)ation could be repressed by PARP-1 inhibitor 3-AB. PARP-1 knockdown increased, while LXR agonist T0901317 further increased ABCA1 protein levels. These data indicate that in islet β cells, PARP-1 could also inhibit LXR-mediated ABCA1 expression by interacting with LXR to induce LXRα poly(ADP-ribosyl)ation.

Bariatric surgery can significantly alleviate T2DM, and usually can significantly improve blood glucose levels before weight loss after surgery [47]. Peterli et al. [48] found that GLP-1 levels after meals were significantly increased in patients 2 months after SG surgery. Another group reported that GLP-1 was elevated postprandially in diabetic patients 6 weeks after SG surgery and maintained for at least 1 year [49]. In the present study, we established STZ-induced T2DM model in SD rats and observed that in T2DM rats, the expression of ABCA1 in the islet tissues was significantly weakened, the cholesterol efflux was blocked, and the cholesterol content in the tissues was significantly increased. On the contrary, RYGB surgery or EX-4 treatment improved the glucose metabolism and lipid metabolism. In the meantime, in

T2DM rats received RYGB surgery or EX-4 treatment, the expression of GLP-1, ABCA1, and LXRβ was increased, the cholesterol content was decreased, the phosphorylation of AMPK was enhanced, while the protein level of PARP-1 was decreased compared with the T2DM or T2DM + sham groups. The results indicate that GLP-1 upregulation after surgery can upregulate the expression of ABCA1 protein, promote the cholesterol efflux from islet β cells, reduce pancreatic cholesterol content, therefore improving the glucose metabolism and lipid metabolism in T2DM rats. Further clinical data from T2DM patients received LSG surgery also evidenced these findings. In these patients, GLP-1 was significantly increased after LSG surgery, and the increase of GLP-1 was closely related to the improvement of islet function.

# Conclusions

In conclusion, GLP-1 inhibits PARP-1 to protect islet β cell function against cholesterol-induced toxicity *in vitro* and *in vivo* through enhancing cholesterol efflux. GLP-1-induced AMPK and LXR-mediated ABCA1 expression are involved in GLP-1 protective effects.

# Abbreviations

ABC: ATP-binding cassette; ABCA1: ATP-binding cassette transporter A1; GLP-1: glucagon-like peptide-1; GSIS: glucose-stimulated insulin secretion; HDL: high-density lipoprotein; HDL-C: high-density lipoprotein cholesterol; H&E: Hematoxylin and eosin; IHC: Immunohistochemical; IP: Immunoprecipitation; LDL: low-density lipoprotein; LSG: laparoscopic sleeve gastrectomy; LXR: liver X receptor; OGTT: Oral glucose tolerance test; PARP: Poly ADP-ribose polymerase; RCT: reverse cholesterol transport; RYGB: Roux-en-Y gastric bypass; STZ: streptozotocin; TC: total cholesterol; TG: total triglyceride; T2DM: type 2 diabetes.

# Declarations

### Ethical Approval and Consent to participate

All procedures performed in studies involving human participants were in accordance with the ethical standards of the Third Xiangya Hospital, Central South University and with the 1964 Helsinki declaration. Informed consent to participate in the study has been obtained from participants.

### Consent for publication

Consent for publication was obtained from the participants.

### Availability of supporting data

Not applicable.

### Conflict of interest

The authors declare that they have no conflict of interest.

### Funding

This study was supported by Talent project of the Third Xiangya Hospital of Central South University (JY201628).

### Authors' contributions

Rao Li, Xulong Sun, Liyong Zhu made substantial contribution to the conception and design of the work; Pengzhou Li, Weizheng Li analyzed and interpreted the data; Rao Li, Xulong Sun, Shaihong Zhu drafted the manuscript; Lei Zhao, Liyong Zhu, Shaihong Zhu revised the work critically for important intellectual content; Liyong Zhu collected grants; All authors read and approved the final manuscript.

### Acknowledgment

Not applicable.

### Authors' information

First author: Rao Li, mail: xs8083610@163.com; Co-first author: Xulong Sun, mail: fengyunjingji@126.com; Pengzhou Li, mail: lipengzhoulpz@163.com; Weizheng Li, mail: 504961855@qq.com; Lei Zhao, mail: 384613584@qq.com; Shaihong Zhu, mail: shaihongzhu@126.com. Correspondence: Liyong Zhu, Tel: +86-13975879453; mail: zly8128@126.com.

# References

1. Thorens B: The required beta cell research for improving treatment of type 2 diabetes. *J Intern Med* 2013, 274:203-214.
2. Buchwald H, Avidor Y, Braunwald E, Jensen MD, Pories W, Fahrbach K, Schoelles K: Bariatric surgery: a systematic review and meta-analysis. *JAMA* 2004, 292:1724-1737.
3. Kreymann B, Williams G, Ghatei MA, Bloom SR: Glucagon-like peptide-1 7-36: a physiological incretin in man. *Lancet* 1987, 2:1300-1304.
4. Holst JJ: On the physiology of GIP and GLP-1. *Horm Metab Res* 2004, 36:747-754.
5. Meier JJ, Gallwitz B, Salmen S, Goetze O, Holst JJ, Schmidt WE, Nauck MA: Normalization of glucose concentrations and deceleration of gastric emptying after solid meals during intravenous glucagon-like peptide 1 in patients with type 2 diabetes. *J Clin Endocrinol Metab* 2003, 88:2719-2725.
6. Larsen PJ, Fledelius C, Knudsen LB, Tang-Christensen M: Systemic administration of the long-acting GLP-1 derivative NN2211 induces lasting and reversible weight loss in both normal and obese rats. *Diabetes* 2001, 50:2530-2539.
7. Huang CN, Wang CJ, Lee YJ, Peng CH: Active subfractions of Abelmoschus esculentus substantially prevent free fatty acid-induced beta cell apoptosis via inhibiting dipeptidyl peptidase-4. *PLoS One* 2017, 12:e0180285.

8. Brunham LR, Kruit JK, Pape TD, Timmins JM, Reuwer AQ, Vasanji Z, Marsh BJ, Rodrigues B, Johnson JD, Parks JS, et al: Beta-cell ABCA1 influences insulin secretion, glucose homeostasis and response to thiazolidinedione treatment. *Nat Med* 2007, 13:340-347.
9. Ishikawa M, Iwasaki Y, Yatoh S, Kato T, Kumadaki S, Inoue N, Yamamoto T, Matsuzaka T, Nakagawa Y, Yahagi N, et al: Cholesterol accumulation and diabetes in pancreatic beta-cell-specific SREBP-2 transgenic mice: a new model for lipotoxicity. *J Lipid Res* 2008, 49:2524-2534.
10. Xia F, Xie L, Mihic A, Gao X, Chen Y, Gaisano HY, Tsushima RG: Inhibition of cholesterol biosynthesis impairs insulin secretion and voltage-gated calcium channel function in pancreatic beta-cells. *Endocrinology* 2008, 149:5136-5145.
11. Brunham LR, Kruit JK, Verchere CB, Hayden MR: Cholesterol in islet dysfunction and type 2 diabetes. *J Clin Invest* 2008, 118:403-408.
12. Westerterp M, Murphy AJ, Wang M, Pagler TA, Vengrenyuk Y, Kappus MS, Gorman DJ, Nagareddy PR, Zhu X, Abramowicz S, et al: Deficiency of ATP-binding cassette transporters A1 and G1 in macrophages increases inflammation and accelerates atherosclerosis in mice. *Circ Res* 2013, 112:1456-1465.
13. Singaraja RR, Brunham LR, Visscher H, Kastelein JJ, Hayden MR: Efflux and atherosclerosis: the clinical and biochemical impact of variations in the ABCA1 gene. *Arterioscler Thromb Vasc Biol* 2003, 23:1322-1332.
14. Tall AR: Role of ABCA1 in cellular cholesterol efflux and reverse cholesterol transport. *Arterioscler Thromb Vasc Biol* 2003, 23:710-711.
15. Kruit JK, Kremer PH, Dai L, Tang R, Ruddle P, de Haan W, Brunham LR, Verchere CB, Hayden MR: Cholesterol efflux via ATP-binding cassette transporter A1 (ABCA1) and cholesterol uptake via the LDL receptor influences cholesterol-induced impairment of beta cell function in mice. *Diabetologia* 2010, 53:1110-1119.
16. Pieper AA, Brat DJ, Krug DK, Watkins CC, Gupta A, Blackshaw S, Verma A, Wang ZQ, Snyder SH: Poly(ADP-ribose) polymerase-deficient mice are protected from streptozotocin-induced diabetes. *Proc Natl Acad Sci U S A* 1999, 96:3059-3064.
17. Xia Q, Lu S, Ostrovsky J, McCormack SE, Falk MJ, Grant SFA: PARP-1 Inhibition Rescues Short Lifespan in Hyperglycemic C. Elegans And Improves GLP-1 Secretion in Human Cells. *Aging Dis* 2018, 9:17-30.
18. Liu FQ, Zhang XL, Gong L, Wang XP, Wang J, Hou XG, Sun Y, Qin WD, Wei SJ, Zhang Y, et al: Glucagon-like peptide 1 protects microvascular endothelial cells by inactivating the PARP-1/iNOS/NO pathway. *Mol Cell Endocrinol* 2011, 339:25-33.
19. Gongol B, Marin T, Peng IC, Woo B, Martin M, King S, Sun W, Johnson DA, Chien S, Shyy JY: AMPKalpha2 exerts its anti-inflammatory effects through PARP-1 and Bcl-6. *Proc Natl Acad Sci U S A* 2013, 110:3161-3166.
20. Shang F, Zhang J, Li Z, Zhang J, Yin Y, Wang Y, Marin TL, Gongol B, Xiao H, Zhang YY, et al: Cardiovascular Protective Effect of Metformin and Telmisartan: Reduction of PARP1 Activity via the

AMPK-PARP1 Cascade. *PLoS One* 2016, 11:e0151845.

21. Shrestha E, Hussein MA, Savas JN, Ouimet M, Barrett TJ, Leone S, Yates JR, 3rd, Moore KJ, Fisher EA, Garabedian MJ: Poly(ADP-ribose) Polymerase 1 Represses Liver X Receptor-mediated ABCA1 Expression and Cholesterol Efflux in Macrophages. *J Biol Chem* 2016, 291:11172-11184.
22. Bradley D, Conte C, Mittendorfer B, Eagon JC, Varela JE, Fabbrini E, Gastaldelli A, Chambers KT, Su X, Okunade A, et al: Gastric bypass and banding equally improve insulin sensitivity and beta cell function. *J Clin Invest* 2012, 122:4667-4674.
23. Reis CE, Alvarez-Leite JI, Bressan J, Alfenas RC: Role of bariatric-metabolic surgery in the treatment of obese type 2 diabetes with body mass index <35 kg/m2: a literature review. *Diabetes Technol Ther* 2012, 14:365-372.
24. Dixon JB, O'Brien PE, Playfair J, Chapman L, Schachter LM, Skinner S, Proietto J, Bailey M, Anderson M: Adjustable gastric banding and conventional therapy for type 2 diabetes: a randomized controlled trial. *JAMA* 2008, 299:316-323.
25. Nannipieri M, Baldi S, Mari A, Colligiani D, Guarino D, Camastra S, Barsotti E, Berta R, Moriconi D, Bellini R, et al: Roux-en-Y gastric bypass and sleeve gastrectomy: mechanisms of diabetes remission and role of gut hormones. *J Clin Endocrinol Metab* 2013, 98:4391-4399.
26. Laferrere B, Heshka S, Wang K, Khan Y, McGinty J, Teixeira J, Hart AB, Olivan B: Incretin levels and effect are markedly enhanced 1 month after Roux-en-Y gastric bypass surgery in obese patients with type 2 diabetes. *Diabetes Care* 2007, 30:1709-1716.
27. Liu H, Deng H, Zhao Y, Li C, Liang Y: LncRNA XIST/miR-34a axis modulates the cell proliferation and tumor growth of thyroid cancer through MET-PI3K-AKT signaling. *J Exp Clin Cancer Res* 2018, 37:279.
28. Liu Y, Wang Y, He X, Zhang S, Wang K, Wu H, Chen L: LncRNA TINCR/miR-31-5p/C/EBP-alpha feedback loop modulates the adipogenic differentiation process in human adipose tissue-derived mesenchymal stem cells. *Stem Cell Res* 2018, 32:35-42.
29. Sankaranarayanan S, Kellner-Weibel G, de la Llera-Moya M, Phillips MC, Asztalos BF, Bittman R, Rothblat GH: A sensitive assay for ABCA1-mediated cholesterol efflux using BODIPY-cholesterol. *J Lipid Res* 2011, 52:2332-2340.
30. Gatmaitan P, Huang H, Talarico J, Moustarah F, Kashyap S, Kirwan JP, Schauer PR, Brethauer SA: Pancreatic islet isolation after gastric bypass in a rat model: technique and initial results for a promising research tool. *Surg Obes Relat Dis* 2010, 6:532-537.
31. Li J, Murao K, Imachi H, Masugata H, Iwama H, Tada S, Zhang GX, Kobayashi R, Ishida T, Tokumitsu H: Exendin-4 regulates pancreatic ABCA1 transcription via CaMKK/CaMKIV pathway. *J Cell Mol Med* 2010, 14:1083-1087.
32. Rouleau M, Patel A, Hendzel MJ, Kaufmann SH, Poirier GG: PARP inhibition: PARP1 and beyond. *Nat Rev Cancer* 2010, 10:293-301.
33. Oliver FJ, Menissier-de Murcia J, Nacci C, Decker P, Andriantsitohaina R, Muller S, de la Rubia G, Stoclet JC, de Murcia G: Resistance to endotoxic shock as a consequence of defective NF-kappaB

activation in poly (ADP-ribose) polymerase-1 deficient mice. *EMBO J* 1999, 18:4446-4454.

34. Andreone TL, O'Connor M, Denenberg A, Hake PW, Zingarelli B: Poly(ADP-ribose) polymerase-1 regulates activation of activator protein-1 in murine fibroblasts. *J Immunol* 2003, 170:2113-2120.
35. Bai P, Canto C, Oudart H, Brunyanszki A, Cen Y, Thomas C, Yamamoto H, Huber A, Kiss B, Houtkooper RH, et al: PARP-1 inhibition increases mitochondrial metabolism through SIRT1 activation. *Cell Metab* 2011, 13:461-468.
36. Xu G, Stoffers DA, Habener JF, Bonner-Weir S: Exendin-4 stimulates both beta-cell replication and neogenesis, resulting in increased beta-cell mass and improved glucose tolerance in diabetic rats. *Diabetes* 1999, 48:2270-2276.
37. Kwon DY, Kim YS, Ahn IS, Kim DS, Kang S, Hong SM, Park S: Exendin-4 potentiates insulinotropic action partly via increasing beta-cell proliferation and neogenesis and decreasing apoptosis in association with the attenuation of endoplasmic reticulum stress in islets of diabetic rats. *J Pharmacol Sci* 2009, 111:361-371.
38. Murao K, Li J, Imachi H, Muraoka T, Masugata H, Zhang GX, Kobayashi R, Ishida T, Tokumitsu H: Exendin-4 regulates glucokinase expression by CaMKK/CaMKIV pathway in pancreatic beta-cell line. *Diabetes Obes Metab* 2009, 11:939-946.
39. Miyai Y, Murao K, Imachi H, Li J, Nishiuchi Y, Masugata H, Iwama H, Kushida Y, Ishida T, Haba R: Exendin-4 regulates the expression of the ATP-binding cassette transporter A1 via transcriptional factor PREB in the pancreatic beta cell line. *J Endocrinol Invest* 2011, 34:e268-274.
40. Oram JF, Lawn RM: ABCA1. The gatekeeper for eliminating excess tissue cholesterol. *J Lipid Res* 2001, 42:1173-1179.
41. Luu W, Sharpe LJ, Gelissen IC, Brown AJ: The role of signalling in cellular cholesterol homeostasis. *IUBMB Life* 2013, 65:675-684.
42. Robichaud S, Ouimet M: Quantifying Cellular Cholesterol Efflux. *Methods Mol Biol* 2019, 1951:111-133.
43. Henquin JC: Triggering and amplifying pathways of regulation of insulin secretion by glucose. *Diabetes* 2000, 49:1751-1760.
44. Kahn SE: Clinical review 135: The importance of beta-cell failure in the development and progression of type 2 diabetes. *J Clin Endocrinol Metab* 2001, 86:4047-4058.
45. Jagtap P, Szabo C: Poly(ADP-ribose) polymerase and the therapeutic effects of its inhibitors. *Nat Rev Drug Discov* 2005, 4:421-440.
46. Vida A, Marton J, Miko E, Bai P: Metabolic roles of poly(ADP-ribose) polymerases. *Semin Cell Dev Biol* 2017, 63:135-143.
47. Madsbad S, Dirksen C, Holst JJ: Mechanisms of changes in glucose metabolism and bodyweight after bariatric surgery. *Lancet Diabetes Endocrinol* 2014, 2:152-164.
48. Peterli R, Wolnerhanssen B, Peters T, Devaux N, Kern B, Christoffel-Courtin C, Drewe J, von Flue M, Beglinger C: Improvement in glucose metabolism after bariatric surgery: comparison of laparoscopic

Roux-en-Y gastric bypass and laparoscopic sleeve gastrectomy: a prospective randomized trial. *Ann Surg* 2009, 250:234-241.

49. Papamargaritis D, le Roux CW, Sioka E, Koukoulis G, Tzovaras G, Zacharoulis D: Changes in gut hormone profile and glucose homeostasis after laparoscopic sleeve gastrectomy. *Surg Obes Relat Dis* 2013, 9:192-201.

# Table

**Table 1 Changes of metabolic parameters in patients before and after LSG**

| Variables | baseline | after surgery |
|---|---|---|
| Fasting GLP-1 (pmol/l/min) | 5.0(4.1) | 6.1(5.6) |
| 30min GLP-1 (pmol/l/min) | 5.8 (3.0) | 8.5 (2.9) * |
| Fasting Insulin (mU/l/min) | 7.6(3.7) | 4.9(8.5)* |
| Fasting Glucose (mmol/l/min) | 8.4(4.4) | 6.3(3.6)* |
| 2h Glucose (mmol/l/min) | 15.9 (8.6) | 10.2 (3.8) * |
| Fasting C-peptide (ng/ml /min) | 2.3(5.1) | 1.6(2.7)* |
| DI | 0.35(2.4) | 2.4(6.5)* |
| IAI | 0.02(0.06) | 0.03(0.01) |
| Insulinogenic index | 1.5(1.4) | 6.8(1.3)* |
| HOMA-β | 3.6(1.6) | 6.5(0.8)* |
| BMI ($kg / m^2$) | 34.1(5.9) | 28.5(5.2) * |
| HbA1c (%) | 7.6(4.6) | 6.3(3.5) * |

* Compared with that before LSG surgery, $P < 0.05$.

# Figures

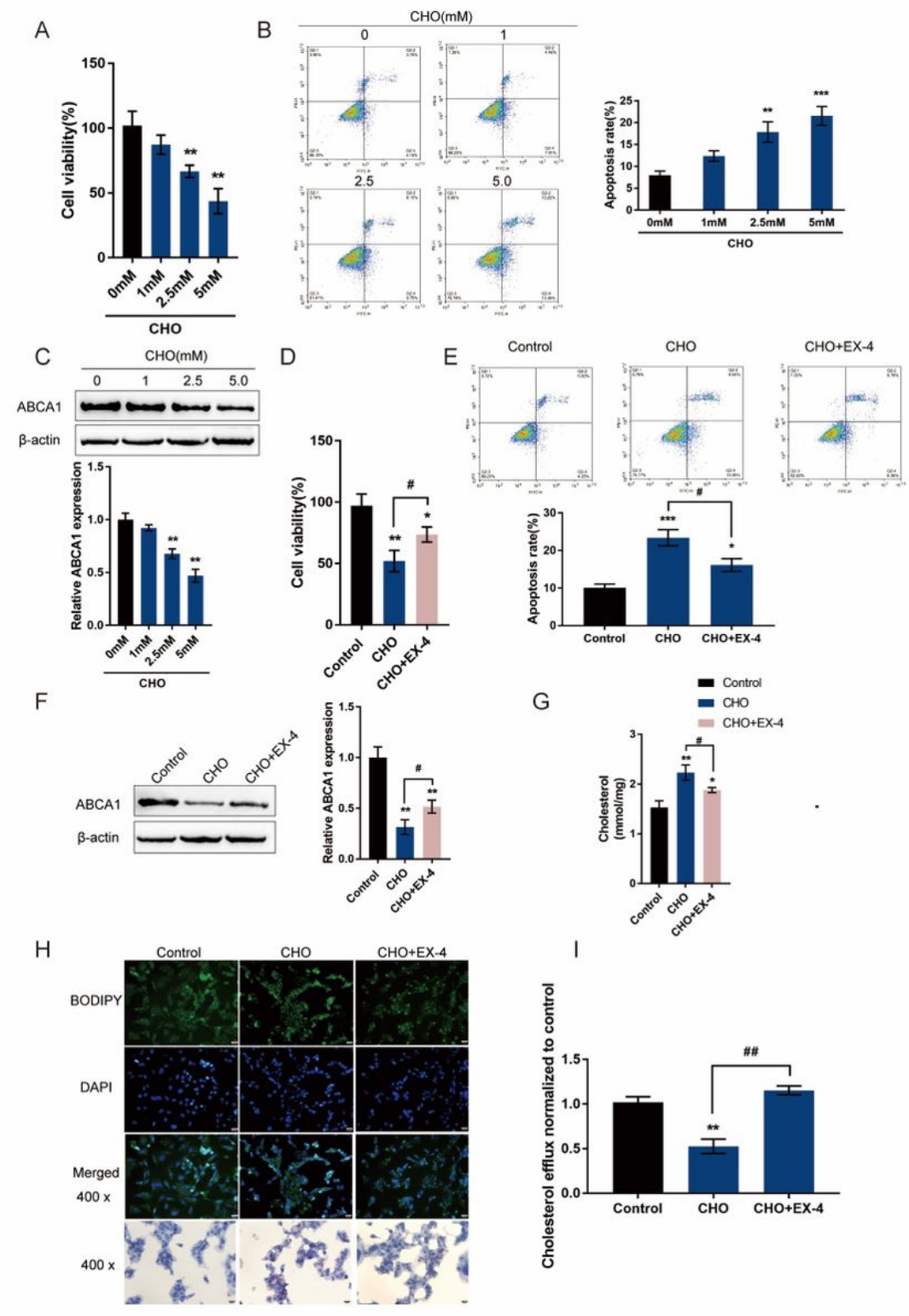


## Figure 1

GLP-1 downregulates ABCA1 expression and cholesterol accumulation-induced toxicity in INS-1 cells INS-1 cells were cultured in medium containing a series of concentrations of cholesterol (0, 1, 2.5, and 5 mM) for 24 h and examined for (A) cell viability by MTT assay; (B) cell apoptosis by Flow cytometry; (C) the protein levels of ABCA1 by Immunoblotting. Next, INS-1 cells were cultured in medium containing 5 mM cholesterol in the presence or absence of 5 nM Exendin-4 (EX-4) for 24 h and examined for (D) cell

viability by MTT assay; (E) cell apoptosis by Flow cytometry; (F) the protein levels of ABCA1 by Immunoblotting; (G) intracellular cholesterol concentration using cholesterol assay kits; (H) intracellular lipid deposition by Oil Red O and BODIPY staining. (I) the cholesterol efflux from INS-1 cells by BODIPY-cholesterol assay; *P<0.05, **P<0.01, ***P<0.005, #P<0.05.

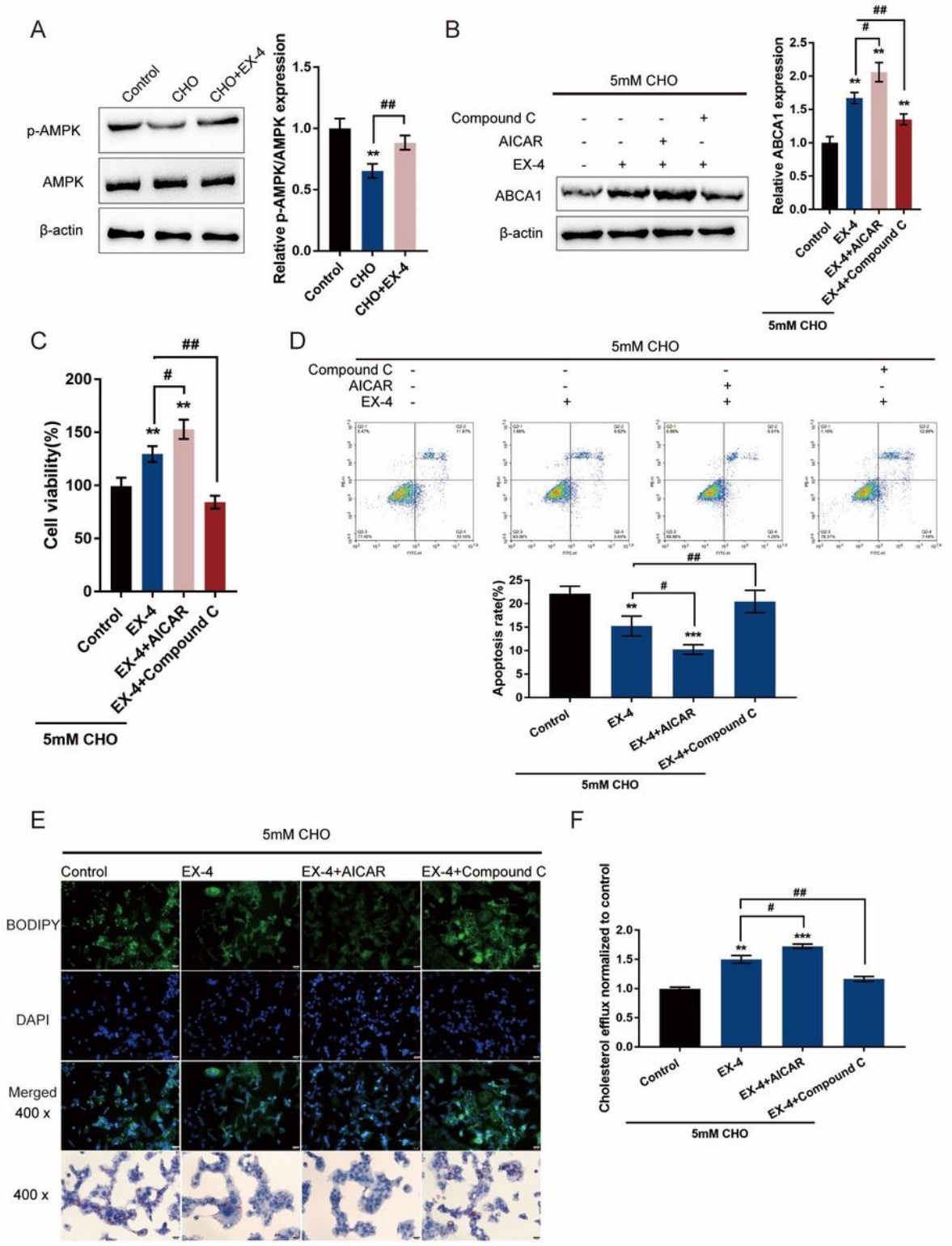


Figure 2

AMPK signaling is involved in GLP-1 regulation of ABCA1 expression and cholesterol-induced toxicity (A) INS-1 cells were cultured in medium containing 5 mM cholesterol in the presence or absence of 5 nM EX-4 for 24 h and examined for the protein levels of p-AMPK and AMPK by Immunoblotting. Next, INS-1 cells were treated with EX-4 in the presence of AMPK activator AICAR or AMPK inhibitor Compound C under the stimulation of cholesterol and examined for (B) the protein levels of ABCA1 by Immunoblotting; (C) cell viability by MTT assay; (D) cell apoptosis by Flow cytometry; (E) intracellular lipid deposition by Oil Red O and BODIPY staining. (F) the cholesterol efflux from INS-1 cells by BODIPY-cholesterol assay; **P<0.01, ***P<0.005, #P<0.05, ##P<0.01.

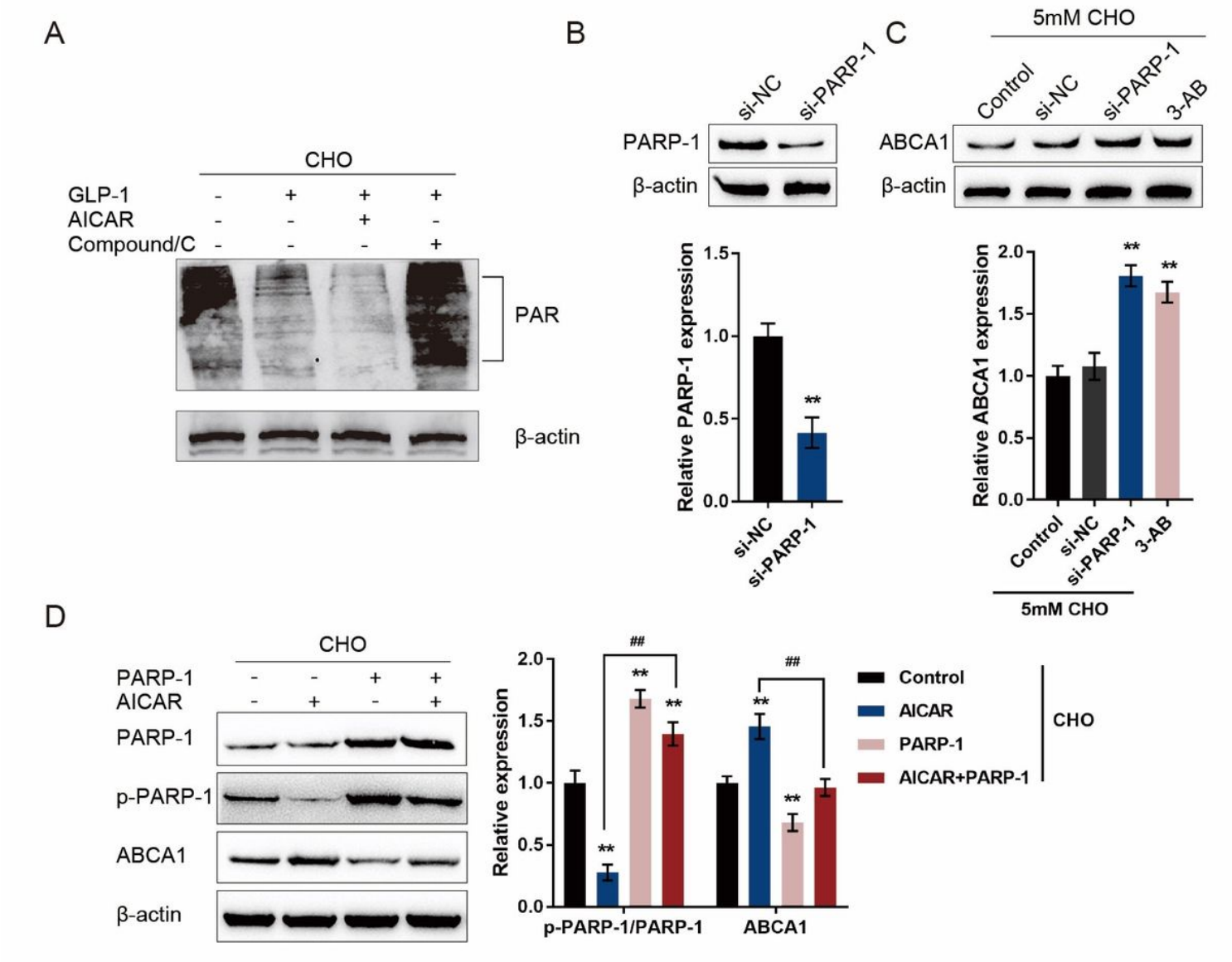


## Figure 3

GLP-1 regulates ABCA1 expression through AMPK-dependent inhibition on PARP1 activity (A) Cholesterol-stimulated INS-1 cells were pre-treated with AMPK activator AICAR or AMPK inhibitor Compound C for 4 h before the addition of GLP-1 and incubated for another 24 h. The protein levels of PAR in INS-1 cell lysates was determined by Immunoblotting. (B) PARP-1 knockdown was generated in INS-1 cells by the transfection of si-PARP-1. The transfection efficiency was confirmed by Immunoblotting. (C) Cholesterol-

stimulated INS-1 cells were transfected with si-PARP-1 or treated with PARP-1 inhibitor 3-AB and examined for the protein levels of ABCA1 by Immunoblotting. (D) Cholesterol-stimulated INS-1 cells were treated with AMPK activator AICAR or PARP-1 alone or co-treated with AICAR and PARP-1 and examined for the protein levels of p-PARP-1 and ABCA1 by Immunoblotting. **P<0.01, ##P<0.01.

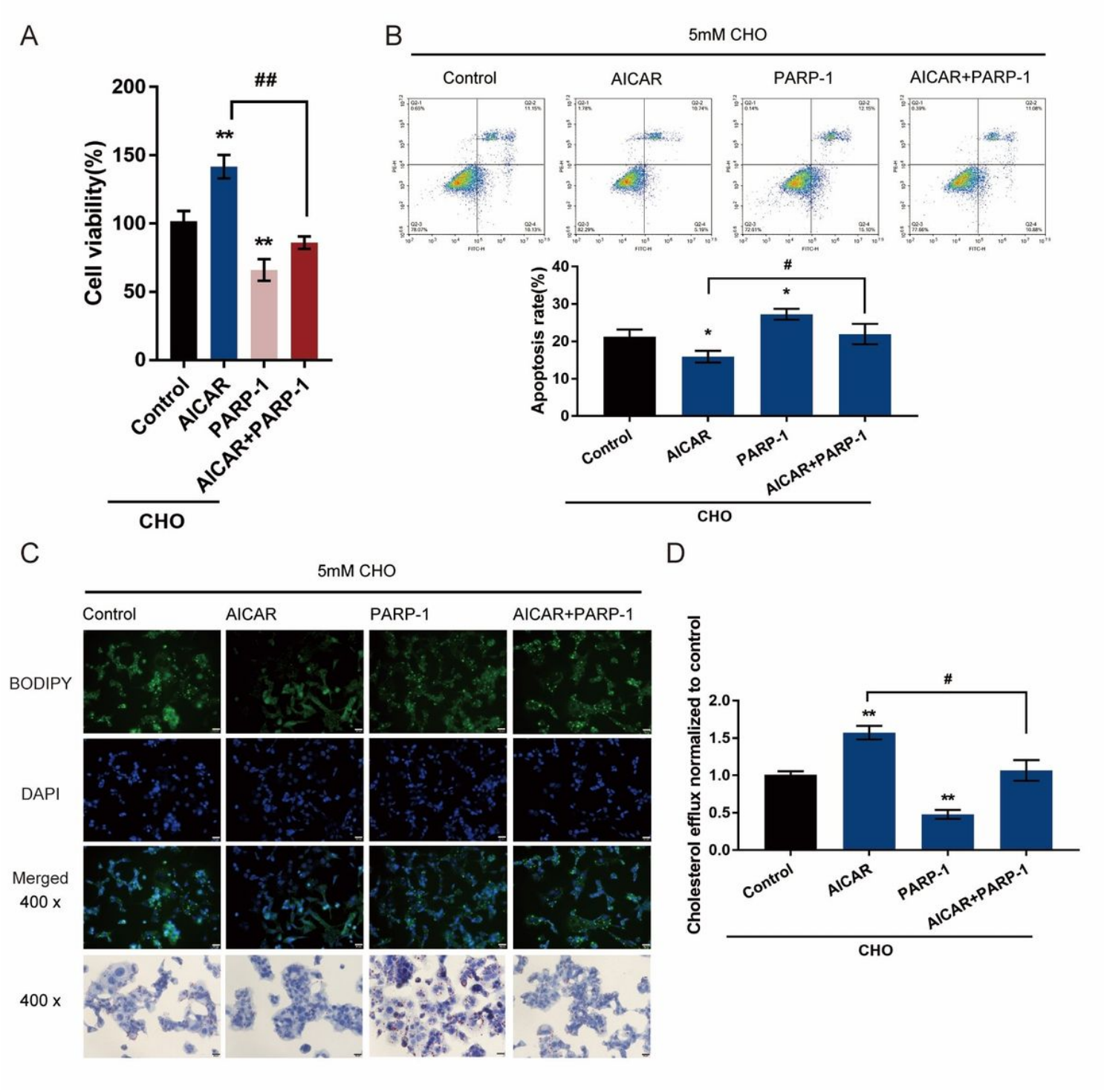


## Figure 4

AMPK inhibits PARP1 activity to attenuate cholesterol-induced toxicity Cholesterol-stimulated INS-1 cells were treated with AICAR or PARP-1 alone or co-treated with AICAR and PARP-1 and examined for (A) cell viability by MTT assay; (B) cell apoptosis by Flow cytometry; (C) intracellular lipid deposition by Oil Red O

and BODIPY staining. (D) the cholesterol efflux from INS-1 cells by BODIPY-cholesterol assay;. *P<0.05, **P<0.01, #P<0.05, ##P<0.01.

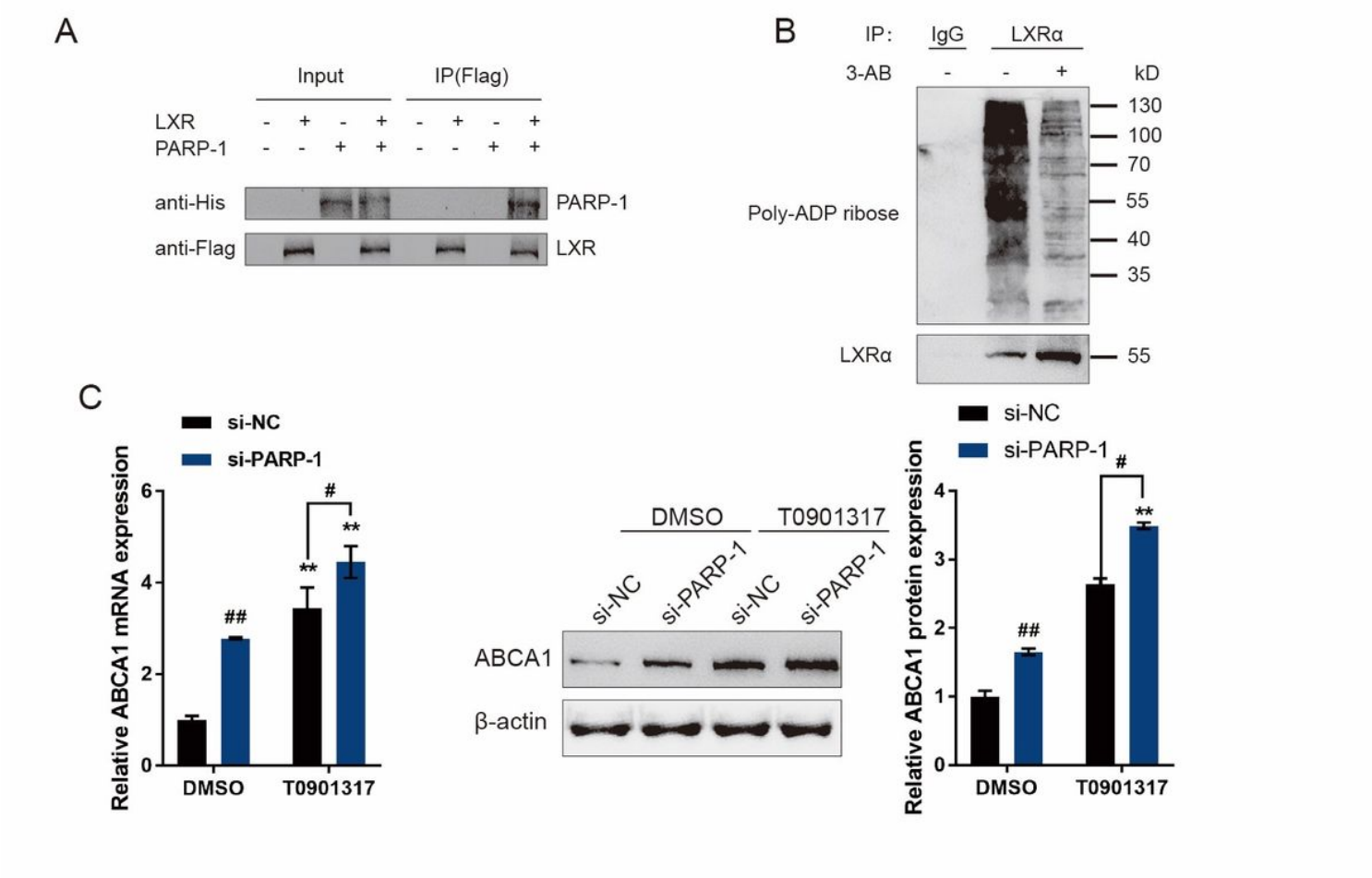


## Figure 5

PAPR-1 inhibits LXR-induced ABCA1 transcription in INS-1 cells (A) Confirmation of the interaction between LXR and PARP-1 in INS-1 cells using coimmunoprecipitation (Co-IP) assay. (C) INS-1 cells were transfected with si-PARP-1 in the presence or absence of LXR receptor agonist T0901317 and examined for the expression and protein levels of ABCA1 by real-time PCR and Immunoblotting. **P<0.01, #P<0.05.

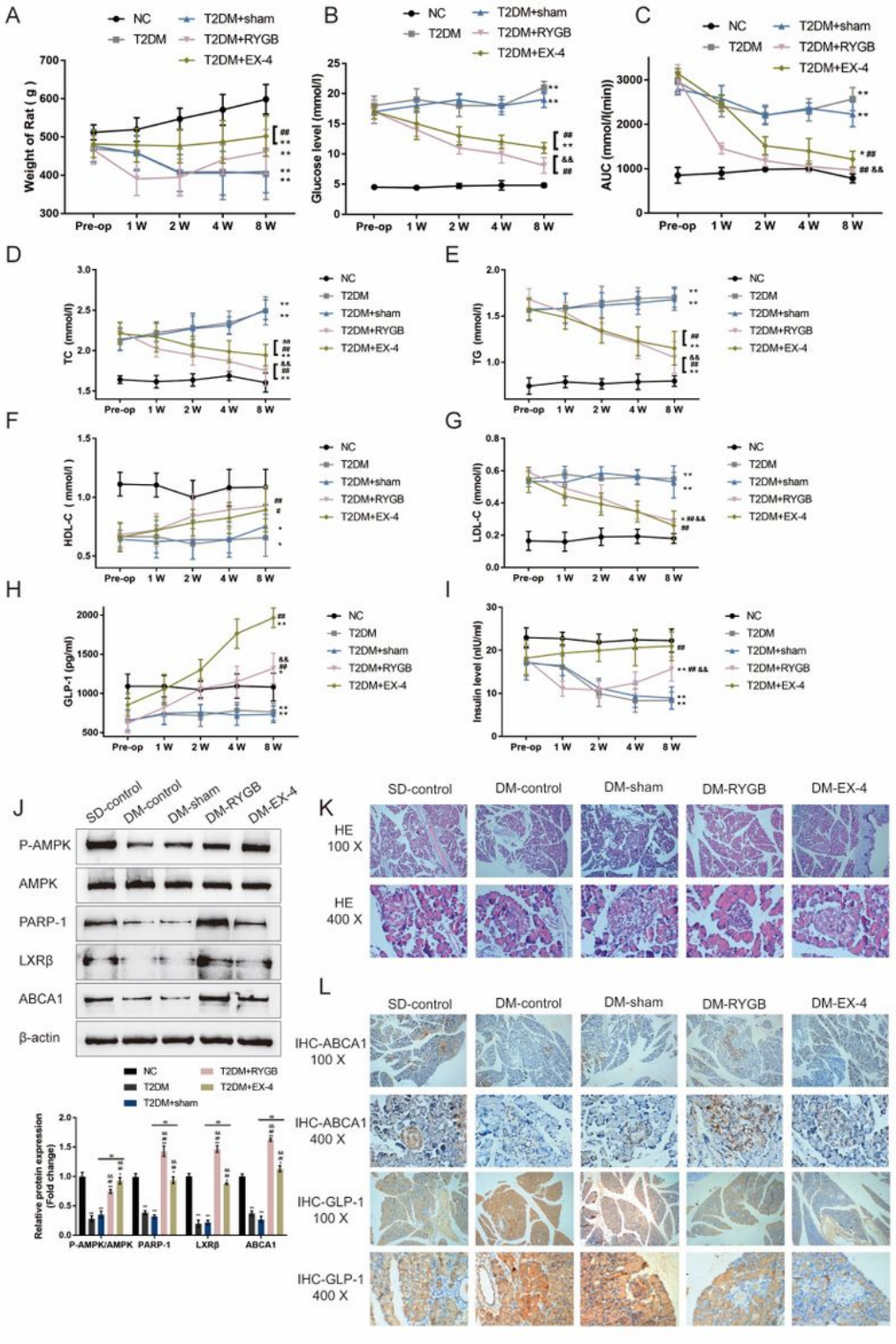


## Figure 6

GLP-1 inhibits PARP-1 to improve islet function in T2DM rats Sprague-Dawley (SD) rats were randomly assigned into five groups: non-treatment control group, streptozotocin (STZ)-induced T2DM group, STZ-induced T2DM plus sham surgery group, STZ-induced T2DM plus RYGB surgery group, and STZ-induced T2DM plus EX-4 treatment group. At pre-operation, 1, 2, 4, and 8 weeks after the last EX-4 treatment, the body weight (A), fasting blood glucose levels (FBG) (B), the area under the curve (AUC) for the OGTT (oral

glucose tolerance test, mmol/L/hour) (C), total cholesterol (TC) (D), triglyceride (TG) (E), low-density lipoprotein cholesterol (LDL-C) (F), and high-density lipoprotein cholesterol (HDL-C) (G), GLP-1 levels (H), and insulin levels (I) were examined. (J) The protein levels of p-AMPK, AMPK, PARP-1, LXRβ, and ABCA1 were examined by Immunoblotting in rats' pancreatic tissues. (K) The histopathology of rats' pancreatic tissues was examined by H&E staining. (L) The protein contents and distribution of ABCA1 and PARP-1 were examined by IHC staining in rats' pancreatic tissues. *P<0.05, **P<0.01, #P<0.05, ##P<0.01, &&P<0.01.

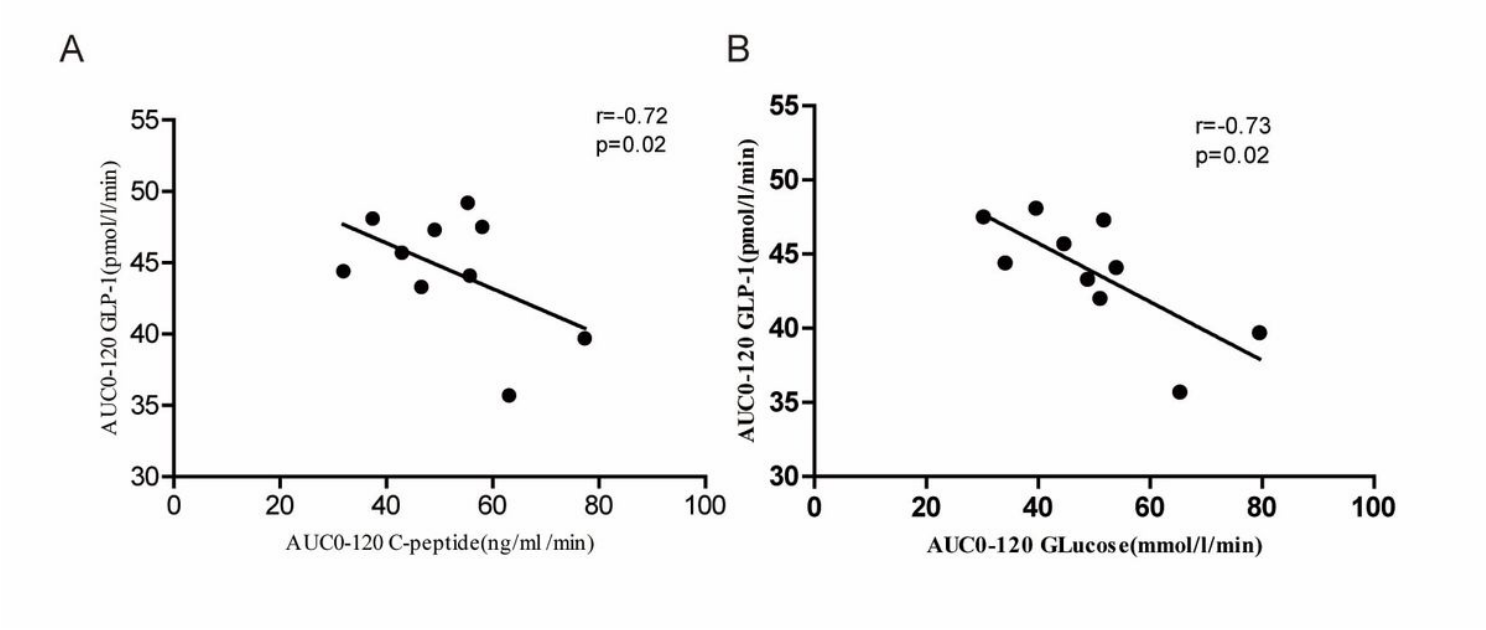


## Figure 7

GLP-1 expression is correlated with islet function after laparoscopic sleeve gastrectomy (LSG) Ten cases of T2DM patients received LSG treatment were enrolled. Three months after and before sleeve gastrectomy, the correlation between the area under the curve of glp-1 and the area under the curve of blood glucose (B) and c-peptide (A) was analyzed.